

PHOTOPRODUCTION OF CHARMONIUM IN A GLUON-EXCHANGE MODEL*

B. Humpert

Stanford Linear Accelerator Center
Stanford University, Stanford, California 94305

ABSTRACT

A model describing photoproduction of a heavy fermion pair which interacts by the exchange of gluons with the target is considered in the framework of the Cheng-Wu picture. Its characteristics are presented and it is applied to ψ_c and η_c photoproduction where the heavy quarks are assumed to be produced in the target's gluon potential. The angular distribution of orthocharmonium reveals a characteristic zero point at $\sqrt{-t} = 2m_c$ whereas the angular distribution of paracharmonium is flat. Arguments and estimates are given for the neglect of the gluon tree diagrams. The model applied to electromagnetic production of $(\tau^+ \tau^-)$ shows that the inclusion of multiphoton exchanges enhances the cross sections by a factor 2-3.

(Submitted to Phys. Rev. D.)

*Work supported by the Energy Research and Development Administration.

I. INTRODUCTION

Photoproduction of a pair of bound heavy quarks ("charmonium") presents the attractive opportunity of studying several theoretical assumptions in strong interaction dynamics which so far have escaped direct insight. The interaction between the quarks is supposed to occur through the exchange of gluons. In analogy to weak and electromagnetic interactions, the strong forces are assumed to be correctly described by a non-Abelian gauge theory whose interaction strength decreases with increasing gluon mass.¹ Consequences of such a viewpoint² are at present subject to extensive phenomenological investigation which have led to a number of characteristic and measurable predictions concerning hadron multiplicity,³ large p_t reactions⁴ and the existence of jets.⁵

The binding of the quarks into physically detectable particles and the non-existence of free quarks is attributed to the confinement mechanism⁶ which allows the quarks to appear as quasifree objects at short distances. The reason for the large mass of the charmed quarks⁷ is another mystery which we have to take as a phenomenological fact which however permits further study, and tests of our present understanding of strong interaction dynamics. Apart from these conceptual theoretical questions, there are a number of phenomenological features in ψ photoproduction⁸ which are substantially different from photoproduction of the conventional vector mesons ρ , ω and ϕ . One wonders why ψ photoproduction is suppressed in comparison to photoproduction of the light-quark vector mesons and why its angular distribution is less peaked in forward direction.⁹

In this paper we investigate the consequences of the non-Abelian gauge theory picture of strong interaction dynamics¹ assuming that the interactions between the quarks are mediated by colored gauge bosons. In particular we study the photoproduction of a heavy quark pair which subsequently undergoes

interaction with the conventional quarks via gluon exchange and eventually forms the bound state $\psi(c\bar{c})$. The most crucial assumption is the validity of a perturbative determination of the scattering amplitude which is motivated at large space-like momenta by the renormalization group results commonly termed as "asymptotic freedom". Measurable consequences of such a point of view have been found in an analysis of the spin dependence of ψ photoproduction.¹⁰ Here rather, we will concentrate on the angular distribution of such a process and its parastate analogue. First results have been reported earlier¹¹ and we here present our complete analysis. Photoproduction of a fermion pair within the framework of quantum electrodynamics has been studied extensively by Cheng and Wu,¹² whose approach we follow closely, and a number of other authors.¹³

The main consequences of the picture sketched above will be studied in a simple model which, we believe, makes obvious many of the features characteristic of our general framework. We will consider the scattering process of a photoproduced heavy quark pair in a scalar $1/r$ (long range) gluon potential due to the target nucleon. The bound state nature of the quark pair is taken into account in the formal presentation of the model but we ignore it in the numerical computations as we wish to focus upon the phenomenological consequences of the gluon exchange picture.

The main question we ask in this work is: What implications has gluon exchange for the angular distribution? The paper is organized as follows: In Section II we give a short introduction to the basic assumptions of QCD and the perturbative recipes for its phenomenological applications.¹² Section III is intended as a brief summary of the infinite momentum frame calculus.¹⁴ The general form of the scattering amplitude with the (fluctuation) wave functions of the photon and the quark bound state is introduced in Section IV. Its structure

is analyzed in Section V and it is cast into an easily calculable form which is used for the evaluation of our numerical results; these are presented and discussed in Section VI. We have determined the cross sections for photoproduction of ψ_c and η_c as well as the photoproduction of an unbound heavy lepton pair $\tau^+ \tau^-$.¹⁵ The application of this model to photoproduction of quark pairs involves the neglect of gluon tree diagrams which, as we are able to show in Section VII, is well justified. Our results and conclusions are summarized in Section VIII.

II. THE GLUON APPROACH

The successes of non-Abelian gauge theories in unifying weak and electromagnetic interactions and the continuing attempts at a more general framework unifying weak, electromagnetic and strong interactions¹ lead us to pursue the dynamical consequences of a field theory of the non-Abelian type in strong interaction dynamics. Its most important characteristic are the gluons being exchanged between the quarks. Much recent study of the phenomenological consequences of such an assumption has been devoted for instance to large- p_t reactions,⁴ to the scaling violation of lepton and hadron induced deep inelastic reactions¹⁶ and most recently to the study of the Pomeron.² Before going into the details of our work, we would like to sketch the most important assumptions and perturbative recipes for quark-gluon theories.

What are the main requirements one would expect of such a theory? The conditions generally agreed upon are (for the hadronic sector)¹:

- (i) renormalizability
- (ii) conservation of parity, isospin, ...
- (iii) asymptotic freedom

- (iv) no strongly interacting scalar fields
- (v) color confinement.

The first condition follows as one desires a calculable descriptive framework which leads to no nonmanageable infinities. Phenomenology leads us to impose condition (ii). As a consequence gluons are polar vectors and all fermions have equal parity under strong interactions. Condition (iii) follows from the non-Abelian character of gauge theories, leading to a $\beta(g)$ opposite in sign relative to Abelian theories (for small g).¹⁷ Again phenomenology imposes condition (iv) whereas (v) is a consequence of the fact that no free quarks and gluons have been seen to date.

The large coupling constant in any field theory describing strong interactions raises the question of whether the apparatus of perturbation theory is applicable. Here we will ignore this problem and assume that indeed a perturbative recipe for quark-gluon theories is applicable. Nussinov² has developed a practical approach for this purpose using the following assumptions:

- (i) The multi-Regge and quark-gluon descriptions are equivalent in the Regge region.
- (ii) Planar duality holds and the simple quark picture of bosons and baryons is correct.
- (iii) Gluon exchanges can be treated perturbatively; but binding into color singlet states has to be treated differently.

Nussinov (and also Low)² recently presented a description of hadronic interactions and in particular their Regge characteristics based upon these rules.

Figure 1 illustrates the idea. Whenever quarks come close they exchange gluons; these in turn create an internal "quark bubble" which attracts many more gluons. Assuming that gluon exchange can be treated perturbatively, one can, to leading order for each diagram, reproduce Regge asymptotics.

The exponential t -dependence, expected for diffractive processes, is due to the quark-bag interaction in this model, which prevents the quarks from appearing as free objects. As an alternative one might argue that two-gluon exchange may only be considered as an order of magnitude approximation since such diagrams show relatively little t -variation. The diffractive t -dependence then might result from the infinite sum of multigluon exchanges; although it is true in QED, this point of view is an unproved conjecture for QCD. Recently the consequences of the two-gluon exchange picture have been investigated in an extensive study of its spin characteristics in ψ -photoproduction. It was concluded that measurement of the spin density matrix elements in the threshold region can give indications of the existence of gluons.¹⁰

We here adopt the opposite viewpoint by assuming that multigluon exchange leads to the Pomeron-like characteristics. We consider the scattering process of a pair of charmed quarks in a scalar $1/r$ (long range) potential. The bound state nature of the quark-pair is retained in the formal presentation of the model; however, it is ignored in the numerical evaluations since we are mostly concerned here with the consequences of gluon exchange. We first present the form of the scattering amplitude as given by Cheng and Wu.¹⁸ Subsequently, we give the angular distribution of the ortho and para $c\bar{c}$ -states; and, finally, we numerically determine the dependence of the scattering amplitude on the quark mass and study the influence and behavior of the multigluon exchange contributions.

However before embarking upon this program and before deriving the form of the scattering amplitude let us briefly introduce the basics of the infinite momentum frame calculus and with it our notation.

III. THE INFINITE MOMENTUM FRAME

Due to covariance and Lorentz invariance of the S-matrix, the scattering processes can be viewed and described in any Lorentz frame. In particular a Lorentz frame may be chosen where the form of the scattering amplitude reduces to a simpler expression and thus allows greater theoretical intuition: the infinite momentum frame.

The infinite momentum frame variables are defined by

$$(t, x, y, z) \rightarrow \left(\tau \equiv \frac{t+z}{\sqrt{2}}, x, y, Z \equiv \frac{t-z}{\sqrt{2}} \right), \quad \vec{r} \equiv (x, y) \quad (3.1)$$

and similarly for the momenta:

$$(E, p_x, p_y, p_z) \rightarrow \left(\eta \equiv \frac{E+p_z}{\sqrt{2}}, p_x, p_y, H \equiv \frac{E-p_z}{\sqrt{2}} \right), \quad \vec{p} \equiv (p_x, p_y) \quad (3.2)$$

with the convenient transformation properties under Lorentz boosts along the z-axis

$$\eta \rightarrow e^u \eta, \quad H \rightarrow e^{-u} H; \quad (3.3)$$

here $\tanh u = v$ is the relative velocity of the two Lorentz frames. Another interesting characteristic of these new variables is that they reveal a formal analogy with nonrelativistic Galilean mechanics in two dimensions.¹⁴ For example the on-mass shell condition $p^2 \equiv 2\eta H - \vec{p}^2 = m^2$ can be written in the form

$$H = \frac{m^2 + \vec{p}^2}{2\eta} = \frac{\vec{p}^2}{2\eta} + \frac{m^2}{2\eta} \quad (3.4)$$

which clearly indicates the correspondence: $H \leftrightarrow$ energy and $\eta \leftrightarrow$ mass, provided the second term in Eq. (3.4) is interpreted as the potential energy. In these new variables the wave functions are normalized according to

$$\langle \eta', \vec{q}' | \eta, \vec{q} \rangle = (2\pi)^3 2\eta \delta(\eta - \eta') \delta^2(\vec{k} - \vec{k}') (2\pi)^3 \delta \dots \quad (3.5)$$

and the invariant measure reads:

$$\frac{1}{(2\pi)^3} \left(\frac{d\eta}{2\eta}\right) d\vec{q} \quad .$$

Galilean boost invariance demands invariance of the wave functions under $\vec{q} \rightarrow \vec{q} + \eta \vec{v}$ giving for a multiparticle state

$$\begin{aligned} |\eta_\kappa, \vec{\kappa}, \eta_1 \vec{q}_1, \dots\rangle &= |\eta_\kappa, \vec{\kappa} + \eta_\kappa \vec{v}; \vec{q} + \eta_1 \vec{v}, \dots\rangle \\ &= |\beta_i, R_i, R_j\rangle \quad R_i \equiv \vec{q}_i - \beta_i \cdot \vec{\kappa}, \quad \beta_i = \frac{\eta_i}{\eta_\kappa} \end{aligned} \quad (3.6)$$

IV. THE SCATTERING AMPLITUDE

Following the approach presented in Section II, the scattering process as described in Fig. 2 occurs in three steps: First, the incoming physical photon fluctuates into a system of freely moving constituents (c-quarks), the partons in the DLY approach.¹⁹ Second, each individual constituent undergoes instantaneous, elastic multiscattering processes in the gluon potential of the nucleon. There is no interaction between the quarks during this process. Finally, they interact to form the observed bound state. Within the gluon exchange framework, this three-step picture is expected to be valid at high energies where the fluctuation lifetime is much larger than the time needed for the interaction with the external gluon potential.

This picture has been elegantly formulated by Bjorken, Kogut and Soper¹⁴ using the infinite momentum frame calculus. The determination of the scattering amplitude requires consideration of the fluctuation wave functions due to the photon, the quark-pair bound state and the amplitude describing the actual gluon scattering process.

A. The Photon Fluctuation Wave Function

In the spirit of the parton approach, we assume that the initial photon state is expanded in a complete set of 'bare' states $\bar{1}$ —the bare photon and the partons—and write:

$$|\gamma\rangle = |\bar{\gamma}\rangle + \int \sum d\Gamma_{12} \cdot M_{12}^\gamma |\bar{1}\rangle \cdot |\bar{2}\rangle + \dots \quad (4.1)$$

where

$$d\Gamma_{12} = \frac{d\vec{\ell}_1}{(2\pi)^3} \frac{d\eta_1}{2\eta_1} \cdot \frac{d\vec{\ell}_2}{(2\pi)^3} \frac{d\eta_2}{2\eta_2} (2\pi)^3 \delta(\eta - \eta_1 - \eta_2) \delta^2(\vec{L} - \vec{\ell}_1 - \vec{\ell}_2) \cdot \sqrt{2\eta_1 2\eta_2} \quad (4.2)$$

stands for the phase space integration over the intermediate parton states which are characterized by their transverse momenta $\vec{\ell}_i$, longitudinal momentum fractions η_i , spin s_i and all other quantum numbers. Since we are working on lowest order electromagnetic interactions only the two parton intermediate state is relevant here. The photon fluctuation wave function is in principle a function of the total momentum $\vec{L} = \vec{\ell}_1 + \vec{\ell}_2$, $\eta = \eta_1 + \eta_2$ and also depends on the momentum components of the two intermediate partons; but it can easily be shown to depend only on the variable combinations

$$\vec{p} = \vec{\ell}_1 \cdot \beta_2 - \vec{\ell}_2 \cdot \beta_1 ; \quad \beta = \frac{1}{2}(\beta_1 - \beta_2) \quad (4.3)$$

because of Galilean invariance. Thus to perform a Lorentz transformation is to change the variable \vec{p} and β . The explicit form of the fluctuation wave functions in lowest order QED have been determined in Ref. 14 using standard rules of the old-fashioned perturbation theory for time-ordered Feynman diagrams with

$$\sqrt{2\eta_1 2\eta_2} \cdot M^\gamma = -e \cdot \frac{\bar{u}_1 \not{\epsilon} v_2}{H - H_1 - H_2} \quad (4.4)$$

H and $H_{1,2}$ are the Hamiltonians of the bare photon and parton states in the infinite momentum frame and \bar{u}_1 and v_2 represent the spinors of the fermions.

For explicit spin combinations we have:

$$M_{\pm 1, \pm\pm}^{\gamma}(\vec{p}, \beta) = e \cdot \frac{m}{m^2 + p^2} \sqrt{2} \quad (4.5)$$

$$M_{+1, \pm\mp}^{\gamma}(\vec{p}, \beta) = \pm e \cdot \left(\frac{1}{2} \pm \beta\right) \frac{p_+}{m^2 + p^2} \sqrt{2} \quad (4.6)$$

$$M_{-1, \pm\mp}^{\gamma}(\vec{p}, \beta) = \pm e \cdot \left(\frac{1}{2} \mp \beta\right) \frac{p_-}{m^2 + p^2} \sqrt{2} \quad (4.7)$$

$$M_{\pm 1, \mp\mp}^{\gamma}(\vec{p}, \beta) = 0 \quad (4.8)$$

where $p_{\pm} = p_x \pm ip_y$.

B. Quark Fluctuation Wave Function

In a completely analogous manner the final state $|\psi\rangle$ is expanded in parton-antiparton states (where here however no bare $|\bar{\psi}\rangle$ -state is allowed since ψ is a bound state of a pair of quarks)

$$|\psi\rangle = \int \sum d\Gamma_{12} \cdot M_{12}^{\psi} \cdot |\bar{1}\rangle |\bar{2}\rangle + \dots \quad (4.9)$$

with the ψ -fluctuation wave function $M_{12}^{\psi}(\vec{p}', \beta')$ being dependent on the momenta of the parton states $|\bar{1}\rangle$ and the total momentum $\vec{L}' = \vec{l}'_1 + \vec{l}'_2$, $\eta' = \eta'_1 + \eta'_2$ as defined in Eq. (3.2). Following Cheng and Wu¹⁸ we relate the bound state fluctuation wave function $M^{\psi}(\vec{p}', \beta')$ to the ordinary Schroedinger bound state wave function $\phi_B(p)$ and describe the bound quark pair by

$$M^{\psi}(\vec{p}', \beta') = \sqrt{2M_B} \cdot \phi_B(\vec{p}', M_B \cdot \beta') C\left(\frac{1}{2}, \lambda_1, \frac{1}{2}, \lambda_2/s', \lambda'\right) \quad (4.10)$$

M_B is the mass of the bound state system, s and λ' are its spin and helicity and λ_1, λ_2 are the helicities of the partons. $C(\dots/\dots)$ stands for the Clebsch-Gordan coefficient. The Schroedinger wave function is normalized as usual:

$$\int \frac{d^3p}{(2\pi)^3} |\phi_B(\vec{p})|^2 = 1 \quad (4.11)$$

The above ansatz (4.10) is well justified as long as the quark masses are heavy and binding energy is small. The factorization of the spin part from the space part in M^ψ is a good approximation if the internal motion of the partons can be neglected and thus the appropriate Wigner rotation for spin projections onto the z-axis may be neglected. If for example a $1/r$ potential between the quarks is assumed the bound state wave function reads²⁰:

$$\phi_B(\vec{p}) \propto \frac{\sqrt{a_0^3}}{(1+a_0^2 \vec{p}^2)^2} \quad a_0 \equiv \frac{2}{m\alpha_s} \quad (4.12)$$

where a_0 is the radius of the bound state and $\alpha_s \equiv g_s^2/4\pi$ is the strong coupling constant.

C. Scattering Amplitude

We are now in a position to specify the scattering amplitude. We sandwich the scattering operator R (defined in $S=1+i\cdot R$) between the wave functions $|\psi\rangle$ and $|\gamma\rangle$ and obtain for the T-matrix the well known result

$$T_{\lambda\lambda'}(\vec{u}) = \int \frac{d\vec{q}}{(2\pi)^2} \left[F_-(\vec{u}+\vec{q}) F_+(\vec{u}-\vec{q}) - (2\pi)^4 \delta^2(\vec{u}+\vec{q}) \delta^2(\vec{u}-\vec{q}) \right] \cdot J_{\lambda'\lambda}(\vec{u}, \vec{q}), \quad (4.13)$$

where $(\vec{p}_i - \vec{p}_f) \equiv 2\vec{u}$ and \vec{p}_i (\vec{p}_f) represents the transverse momentum of the initial γ -state (final ψ -state) and $t = -(\vec{p}_i - \vec{p}_f)^2$. The "impact factor" $J_{\lambda'\lambda}$ contains all information about the creation process and final state binding of the constituent system through the fluctuation wave functions introduced above:

$$J_{\lambda'\lambda}(\vec{u}, \vec{q}) = \int_{-\frac{1}{2}}^{+\frac{1}{2}} d\beta \int_{-\infty}^{+\infty} \frac{d\vec{\ell}}{(2\pi)^2} \sum M_{\lambda'}^{\psi*}(\vec{\ell}+\vec{m}, \beta) \cdot M_{\lambda}^{\gamma}(\vec{\ell}-\vec{m}, \beta) \quad , \quad (4.14)$$

where $\vec{m} = \frac{1}{2} \vec{q} - \beta \vec{u}$ and the sum extends over the fermion helicities which we have omitted. The differential cross section is

$$\frac{d\sigma}{d\Delta^2} = \frac{1}{(4\pi)^3} \sum_{\lambda, \lambda'} |T_{\lambda, \lambda'}|^2 \quad . \quad (4.15)$$

The S-matrix amplitude describing the interaction of each constituent with the gluon potential is parametrized by the eikonal form

$$F_{\pm}(\vec{q}) = \int_{-\infty}^{+\infty} d\vec{b} \cdot e^{-i\vec{q} \cdot \vec{b}} \cdot e^{\pm i\chi(\vec{b})} \quad , \quad (4.16)$$

such that each constituent acquires an eikonal phase shift whereas their longitudinal momenta and helicities remain unchanged.

Let us for later purpose assume a Coulomb-like gluon potential

$$V(r) = \frac{g_s}{4\pi r} \quad (4.17)$$

where g_s stands for the "strong charge". The phase shift $\chi(\vec{b})$ appearing in Eq. (4.16) is related to the potential $V(r)$ by

$$\chi(\vec{b}) = - \int_{-\infty}^{+\infty} dz \cdot g_s \cdot V(\vec{b}, z) \quad (4.18)$$

with the vector $\vec{b} \equiv (b_x, b_y)$ in impact parameter space. The integration is easily performed once an auxiliary nonzero photon mass is introduced through a factor $e^{-\mu r}$ to prevent divergence of the integration. Then

$$\begin{aligned} \chi_{\pm}(\vec{b}) &= -g_s^2 \int \frac{d\vec{q}}{(2\pi)^2} \frac{e^{i\vec{b} \cdot \vec{q}}}{q^2 + \mu^2} = -2\alpha_s \cdot K_0(\mu b) \\ &\xrightarrow{\mu \rightarrow 0} -2\alpha_s \left(\ln \left(\frac{\mu b}{2} \right) + \gamma \right) \end{aligned} \quad (4.19)$$

and inserting this into Eq. (4.16) immediately gives the result

$$F_{\pm}(\vec{q}) = \mp i \frac{4\pi\alpha_s}{q} e^{\mp i\Lambda(\mu, \alpha_s)} \quad (4.20)$$

with the phase factor

$$\Lambda(\mu, \alpha_S) = 2 \cdot \left[\alpha_S (\ln \mu + \gamma) + \arg \Gamma(1 + i\alpha_S) \right] \quad (4.21)$$

depending logarithmically on the small photon mass μ . The formalism presented above (Eqs. (4.13)-(4.15)) has been derived in many different ways: for example, by summing the leading asymptotic behavior of Feynman diagrams, through use of nonrelativistic multiparticle wave functions, by using relativistic eikonalization methods and by the application of infinite momentum frame techniques.¹²⁻¹⁴

We therefore do not consider it worthwhile to go into more details here. Instead we are more concerned with the explicit evaluation of the scattering amplitude and the extraction of its dependence on the momentum transfer.

V. EVALUATION OF THE AMPLITUDE

In the preceding section we have assembled all the necessary ingredients for the scattering amplitude and now are concerned with its explicit dependence on the momentum transfer $t \equiv -(\vec{p}_i - \vec{p}_f)^2$.

We start by considering the impact factor Eq. (4.14); its explicit form is

$$J_{\lambda\lambda'} = \int_{-\frac{1}{2}}^{+\frac{1}{2}} d\beta \int \frac{d\vec{\ell}}{(2\pi)^2} \sum M_{\lambda}^{\gamma}(\vec{\ell} - \vec{m}, \beta) \sqrt{2M_B} \phi(\vec{\ell} + \vec{m}, M_B \beta) C(\dots/s', \lambda') \quad (5.1)$$

with \vec{m} given in Eq. (4.14). λ and λ' are the spin of the photon and the final quark-antiquark bound state and \sum stands for the sum over the spins of the intermediate partons. One immediately realizes that the evaluation of the T-matrix is very difficult in general and nonelegant. We therefore ignore the influence of the bound state here and replace the bound state wave function by a delta-function

which permits decomposition of $J_{\lambda\lambda'}$ into a sum of terms

which permits determination of $J_{\lambda\lambda'}$ in a simpler form:

$$J_{\lambda\lambda'} = \phi_0 \frac{2\pi}{\sqrt{2m}} \left[\sum_{\text{spins}} M_{\lambda}^{\gamma} \cdot C(\dots/s', \lambda') \right] \quad (5.2)$$

By explicit insertion of M_{λ}^{γ} and of the Clebsch-Gordon coefficient it leads to

$$J_{0, \pm 1} = -\phi_0 \cdot 2\pi e \cdot \frac{q_{\pm}}{m^2 + q^2} \cdot \frac{1}{\sqrt{m}} \quad (5.3)$$

$$J_{\pm 1, \pm 1} = +\phi_0 \cdot 2\pi e \cdot \frac{m}{m^2 + q^2} \sqrt{\frac{2}{m}} \quad (5.4)$$

where

$$\phi_0 = \int \frac{d^3 p}{(2\pi)^3} \phi(\vec{p}) \quad (5.5)$$

is the bound state wave function at the origin.

We are now in a position to specify the T-matrix elements by inserting Eqs. (5.3) and (5.4) into Eq. (4.13). By defining the amplitudes for ortho and para charmonium production

$$T^1 \equiv T_{\pm 1, \pm 1} = \sqrt{2} \ r \cdot R^1 \quad (5.6)$$

$$T_{\pm}^0 \equiv T_{0, \pm 1} = r \cdot R^0 \quad (5.7)$$

with

$$r = \left(\frac{8\pi e}{\sqrt{m}} \right) \alpha_s^2 \phi_0 \quad (5.8)$$

we have to determine the t-dependence of the functions

$$R^1(t) = \int_{-\infty}^{+\infty} d\vec{q} \ \xi(\vec{u}, \vec{q}, \alpha_s) \left(\frac{1}{m^2 + q^2} - \frac{1}{m^2 + u^2} \right) \quad (5.9)$$

$$R^0(t) = \int_{-\infty}^{+\infty} d\vec{q} \ \xi(\vec{u}, \vec{q}, \alpha_s) \left(\frac{q_{\pm}}{m^2 + q^2} \right) \quad (5.10)$$

where

$$\xi(\vec{u}, \vec{q}, \alpha_s) = \frac{1}{(\vec{u} + \vec{q})} \times \frac{1}{(\vec{u} - \vec{q})} \frac{1}{2(1-i\alpha_s)} \times \frac{1}{2(1+i\alpha_s)} \quad (5.11)$$

is due to the product of form factors. In deriving Eq. (5.9) we have used the "regularized impact factor" and introduced the additional term $1/m^2 + \vec{q}^2$ in order to weaken the divergence of the integrand at $\vec{q} = \pm \vec{u}$; this is allowed since the identity

$$\int d\vec{q} \left[F_-(\vec{q} + \vec{u}) F_+(\vec{q} - \vec{u}) - (2\pi)^4 \delta^2(\vec{u} + \vec{q}) \delta^2(\vec{u} - \vec{q}) \right] J(\vec{u}, \vec{u}) = 0 \quad (5.12)$$

holds. In order to extract the t-dependence of Eqs. (5.9) and (5.10) we use the generalized Feynman parameter integrals:

$$\frac{1}{a^{1-\gamma}} \frac{1}{b^{1+\gamma}} = \frac{\text{sh} \pi \alpha_s}{\pi \alpha_s} \int_0^1 d\alpha \frac{\alpha^{-\gamma} (1-\alpha)^\gamma}{[\alpha a + (1-\alpha)b]^2} \quad (5.13)$$

and integrate in Eqs. (5.9) and (5.10) over $d\vec{q}$ with the result¹⁸

$$R_{\pm}^0(t) = \frac{\pi}{m^3} \sigma_{\pm} \cdot L^0(\sigma) \quad (5.14)$$

$$R^1(t) = -\frac{\pi}{m^3} \epsilon \cdot L^1(\sigma) \quad (5.15)$$

where

$$L^0(\sigma) = \frac{\text{sh} \pi \alpha_s}{\pi \alpha_s} \cdot \int_0^1 \int d\alpha d\beta \frac{\alpha^{-\gamma} (1-\alpha)^\gamma (1-2\alpha)\beta^2}{[\beta\sigma^2 \cdot F + 1 - \beta]^2} \quad (5.16)$$

$$L^1(\sigma) = \frac{\text{sh} \pi \alpha_s}{\pi \alpha_s} \cdot \int_0^1 \int d\alpha d\beta \frac{\alpha^{-\gamma} (1-\alpha)^\gamma \beta(1-\beta)}{[\beta\sigma^2 \cdot F + 1 - \beta]^2} \quad (5.17)$$

and the functions

$$F \equiv 1 - (1-2\alpha)^2 \beta$$

$$\sigma \equiv \frac{|\vec{u}|}{m} \quad \sigma_{\pm} \equiv \frac{u_x \pm i u_y}{m} \quad \gamma \equiv i\alpha_s \quad (5.18)$$

$$\epsilon \equiv \frac{1-\sigma^2}{1+\sigma^2}$$

have been introduced. Straightforward application of the Mellin transformation techniques permits evaluation of the σ -behavior for small values. The result after a lengthy but straightforward calculation is¹⁸:

$$L^0 = \frac{i}{2\alpha_s} \frac{1}{\sigma^2} \left(\frac{1}{1+\sigma^2} \right) + 4\gamma \left[\text{Re } \psi(1+\gamma) - \psi(1) + \frac{1}{2} \ln 4 \right] + \dots \quad (5.19)$$

$$L^1 = - \left(\frac{1}{1-\sigma^2} \right)^2 \ln \left(\frac{2\sigma}{1+\sigma^2} \right)^2 + \dots \quad (5.20)$$

In evaluating Eqs. (5.16) and (5.17) we have limited ourselves to the most singular terms which correspond to 1, 3, ... gluon exchange for L^0 and to 2, 4, ... gluon exchange for L^1 . This is consistent with C-invariance which requires that an even number of gluons be exchanged for ortho charmonium and an odd number for para charmonium. Since color conservation forbids single gluon exchange the first contribution to L^0 in Eq. (5.19) has to be dropped. It represents the Born approximation and would be analogous to Primakoff photoproduction of η_c . L^0 and L^1 can be expressed in closed form as derived in Ref. 21 and also recently discussed in Ref. 22:

$$L^0 = \xi^0 \frac{V(\epsilon^2)}{V(1)}, \quad L^1 = \xi^1 \frac{W(\epsilon^2)}{V(1)} \frac{\epsilon^2}{\ln(1-\epsilon^2)} \quad (5.21)$$

where

$$\xi^0 \equiv \frac{i}{2\alpha_s} \frac{1}{\sigma^2} \left(\frac{1}{1+\sigma^2} \right), \quad \xi^1 \equiv - \left(\frac{1}{1-\sigma^2} \right)^2 \ln \left(\frac{2\sigma}{1+\sigma^2} \right)^2 \quad (5.22)$$

and

$$V(\epsilon^2) \equiv {}_2F_1(-\gamma, \gamma, 1; \epsilon^2); \quad W(\epsilon) \equiv {}_2F_1(1-\gamma, 1+\gamma, 2; \epsilon^2). \quad (5.23)$$

The above derivation is based upon the fact that the binding effect of the produced parton pair may be ignored and thus essentially we determined the production of two free c-quarks which move with the same momentum. Before going to the numerical evaluation and phenomenological discussion of this model we indicate a possible extension of this formalism which accounts for the binding effects. We return to Eq. (4.13) and write it in the form

$$T_{\lambda\lambda'} = \int_{-\infty}^{+\infty} \frac{d\vec{q}}{(2\pi)^2} \xi(\vec{q}, \vec{u}) \cdot J_{\lambda\lambda'}(\vec{q}, \vec{u}) \quad (5.24)$$

where $\xi(\vec{q}, \vec{u})$ is defined in Eq. (4.13) and $J_{\lambda\lambda'}$ for specific helicities may be given by

$$J(\vec{q}, \vec{u}) \equiv \int_{-\frac{1}{2}}^{+\frac{1}{2}} d\beta \int \frac{d\vec{l}}{(2\pi)^2} \frac{(\ell_{\pm})}{m^2 + \vec{l}^2} \phi(\vec{L}, M_B \beta) \Big|_{\vec{L}=\vec{k}+\vec{q}-2\beta\vec{u}} \quad (5.25)$$

Using the Fourier transformed bound state wave function

$$\Phi(\vec{L}) = \int_{-\infty}^{+\infty} \frac{d\vec{r}}{(2\pi)^3} e^{i\vec{L} \cdot \vec{r}} \phi(\vec{r}) \quad (5.26)$$

we may rewrite Eq. (5.24) in the factorized form

$$T = \int_{-\infty}^{+\infty} \frac{d\vec{r}}{(2\pi)^2} I_1(\vec{r}, \vec{u}) \cdot I_2(\vec{r}) \cdot I_3(\vec{r}, \vec{u}) \quad (5.27)$$

where I_1 stands for the interaction between the quarks and the exchanged gluons, I_2 describes the quark creation process and I_3 parametrizes the bound state nature of the quark-antiquark system. The explicit forms are

$$I_1(\vec{r}, \vec{u}) \equiv \int_{-\infty}^{+\infty} d\vec{q} \cdot e^{i\vec{q} \cdot \vec{r}} \cdot \xi(\vec{q}, \vec{u}) \quad (5.28)$$

$$I_2(\vec{r}) \equiv \int_{-\infty}^{+\infty} d\vec{l} \cdot e^{i\vec{l} \cdot \vec{r}} \frac{(\ell_{\pm})}{m^2 + \vec{l}^2}$$

$$I_3(\vec{r}, \vec{u}) \equiv \int_{-\infty}^{+\infty} \frac{dr_3}{(2\pi)} \int_{-\frac{1}{2}}^{+\frac{1}{2}} d\beta \cdot e^{-i\beta(2\vec{u} \cdot \vec{r} - M_B \cdot r_3)} \phi(\vec{r}) \quad (5.30)$$

Further simplification of these expressions is involved. Since our main interest in this paper is in the effects due to gluons we leave the nature of bound state corrections for a later investigation.

VI. NUMERICAL RESULTS

The numerical evaluation of this model is straightforward. Before presenting the results let us first make a few observations about the formulas:

We first consider $c\bar{c}$ -photoproduction in an ortho state like $\rho, \omega, \dots, \psi \dots$. The amplitude $R^1(t)$ has a universal zero at $\sigma=1$ corresponding to $\sqrt{-t} = 2m$ due to the logarithmic term in $L^1(\sigma)$. (This apparent divergence cancels against the zero in ϵ .) This zero is already present in the two-gluon exchange term. Its position in the momentum transfer variable depends upon the mass of the constituents m ; thus if a heavy quark system is produced the minimum lies far out in $-t$ whereas a light quark system has the minimum at lower t -values.

Plotting $-t/4m_c^2$ should then reveal a constant and fixed minimum point at $+1$. We now consider photoproduction of the para $c\bar{c}$ -state. Keeping only the first term in L^0 , we find the Born amplitude of single gluon exchange which however is forbidden by color conservation. It shows an angular distribution with a sharp spike in forward direction, like $1/t$, and which then falls to zero. Both amplitudes R^0 and R^1 depend only on the variable σ and therefore scale in the quark mass if a change in the overall size of the cross section is ignored. Since we are working in the infinite momentum frame, the dependence on the initial energy $E_{c.m.}$ has completely dropped out; our formalism is therefore not valid in the threshold region and is preferentially applied in the asymptotic region

where the diffraction phenomena seem to dominate. The bound state wave function $\phi_0(\alpha_s, m_c)$ most likely depends on the mass of the quarks as well as the strong coupling constant. This dependence is undefined unless a specific choice of the bound-state wave function is made. As an attempt we assume the form resulting from a Coulomb potential

$$\phi_0 = \frac{1}{\sqrt{\pi a_0^3}}, \quad a_0 \equiv \frac{2}{m_c \cdot \alpha_s}, \quad \alpha_s \equiv \frac{g_s^2}{4\pi}. \quad (6.1)$$

Ignoring the mass dependence of the bound state wave function ϕ_0 both amplitudes R^0 and R^1 are proportional to $m_c^{-7/2}$. Note that the above results show no dependence on the target (nucleon) size since we have used an infinitely extended $1/r$ -gluon potential.

We have numerically evaluated the shape of the differential cross section for ψ_c -photoproduction adjusting the bound state wave function at the origin ϕ_0 in Eq. (6.1) by a multiplicative factor such that its size agrees with the data at $E_{c.m.} \sim 120$ GeV. In Fig. 3a we show its shape for $m_c = 1.5$ GeV and $\alpha_s = 0.5$; the analogous curves in Fig. 3c are for $m_q = 0.3$ GeV. The dashed lines (2-gluon exchange) represent the lowest order contribution. The solid lines (2, 4, 6 ... gluon exchanges) take multigluon corrections into account and the dashed-dotted lines (4, 6, ... gluon exchanges) have the 2-gluon exchange subtracted. One notices that the 2-gluon exchange approximation is damped down by the higher order multigluon exchanges which however interfere such that their contribution is about one order of magnitude smaller. An exponential fit in the region $0.1 \leq -t \leq 0.6$ (GeV/c)² gives a slope parameter $b \sim 2-4$ GeV⁻²; it is less for 4, 6, ... gluon exchange. Mass extrapolation to $m_q = 0.3$ GeV (Fig. 3c) brings the zero-point in the amplitude R^1 (see Eq. (5.10)) to

$-t = 0.36 \text{ (GeV/c)}^2$. This diffraction minimum is not observed in ρ -photoproduction²³ and it might disappear if the relativistic bound state nature of the ρ -meson is taken into account.

In Fig. 4a and Fig. 4c we show the analogous curves for photoproduction of the para states η_c and η_q . For illustrative purpose we have drawn the Born-approximation (which however is forbidden by color conservation); it is strongly peaked for small $|t|$ -values. 3,5,... gluon exchange is flat over a long t -range and bends off towards zero in the extreme forward direction. The same calculation with $m_c = 0.3 \text{ GeV}$ shows a rising curve towards smaller $|t|$ -values with $b \sim 5 \text{ GeV}^{-2}$ and a falloff to zero in the extreme forward direction.

In Figs. 3b and 4b the value of the strong coupling constant is changed to $\alpha_s = 0.8$ but the quark mass is kept at $m_c = 1.5 \text{ GeV}$. Comparing Figs. 3a and 3b one notices that the curves rise by a factor 5-10 in going from $\alpha_s = 0.5$ to 0.8. Furthermore the sum of terms describing 4,6,... gluon exchange is much more influential relative to the 2-gluon exchange term. The fact that at larger $(-t)$ -values the 4,6,... gluon exchange and the 2,4,6,... gluon exchange contributions are of similar size is a consequence of the interference pattern between the amplitudes T_2 and $T_{46\dots}$; however, the qualitative shape of the curves changes little. Similar conclusions can be drawn by comparing the diagrams in Figs. 4a and 4b. Again one finds that the relative size of the various contributions becomes narrower. Note in particular that the 3 gluon exchange is of almost equal size as the cross section due to 3,5,... gluon exchange. The trend we see here is that the influence of the multigluon exchange terms is more strongly felt as we increase the coupling strength of the gluonic interaction. It is in agreement with the intuitive expectation that higher order terms become more strongly felt.

So far we have not mentioned the application of the above formalism to the production of a particle system which interacts predominantly by electromagnetic force. Primakoff-photoproduction of an unbound $\tau^+\tau^-$ system (τ^+ and τ^- produced with equal momenta) in the multiple charged field of nuclei is an example. The replacement of the exchanged gluon coupling constant $\alpha_s \rightarrow Z \cdot \alpha$ ($\alpha \equiv e^2/4\pi$, $Z \equiv$ nucleus charge) and explicit calculation shows that the higher order corrections are nonnegligible and in fact enhance the cross section by a factor 2-3.

The production of the unbound $\tau^+\tau^-$ para state in the single photon approximation leads to the familiar form

$$\left(\frac{d\sigma}{dt}\right)_{\text{para}} = 8\pi \alpha^4 (\alpha Z)^2 \frac{m_\tau^2}{t} \left(\frac{1}{t-4m_\tau^2}\right)^2 \quad (6.2)$$

which gives the integrated cross section

$$\sigma_{\text{para}} \cong \frac{\pi}{m_\tau^2} \alpha^4 (\alpha Z)^2 \ln \frac{E_{\text{lab}}}{m_c} \quad (6.3)$$

The differential distribution and integrated cross section for production of the analogous $\tau^+\tau^-$ ortho state is not as suppressed as it might seem by considering the extra factor α^2 (due to the additional photon being exchanged) since the electromagnetic field of the nucleus contributes an additional factor Z . In Figs. 5 we show the shapes and sizes of the differential cross sections. We emphasize that these results may not be applied to "leptonium" photoproduction¹⁵ since we have ignored the electromagnetic binding forces. Since these are very weak, the resulting t -dependent form factor is exponentially damped with a large slope value so that the integrated cross sections are orders of magnitudes below the ones given in Fig. 5.

VII. OTHER DIAGRAMS

In the above analysis we have considered a specific class of gluon exchange diagrams for the description of the interactions between the photoproduced heavy quark pair and the nucleon. Quantum chromodynamics however does permit a much larger class of diagrams which has been ignored so far. In this section we attempt an estimate of the importance and influence of these diagrams. Primarily we wish to know whether the class of diagrams with multigluon couplings as shown in Fig. 6 can be neglected.

To simplify the discussion we ignore any interaction among the two heavy quarks and draw the diagrams with the two quarks leaving in opposite direction (Fig. 7). The class of diagrams contributing to this process is subject to the two constraints:

- (i) The number of gluons attached to the c-quark lines must be even (odd) for ψ_c (η_c) photoproduction due to Furry's theorem (C-parity conservation).
- (ii) The number of gluons which are exchanged between the gluon source and the $c\bar{c}$ -pair must be ≥ 2 due to color conservation.

Let us first consider photoproduction of an ortho bound state. The diagrams contributing in lowest order g_s^4 (the gluon coupling constant), with the gluon lines attached in all possible ways on the quark lines, are indicated in Fig. 8. In next order g_s^6 tree-diagrams such as shown in Fig. 9a are excluded since an un-even number of gluons is attached to the quark lines violating constraint (i). In order g_s^8 the tree-diagram which might spoil our earlier results are of the type shown in Fig. 9b. That these diagrams give contributions which are unimportant is assured by the following two points:

- (a) Since we have carried out all our analysis assuming that

perturbation theory is applicable, the gluon coupling has to be smaller than 1; as a consequence contributions to order g_s^8 are suppressed with respect to order g_s^4 .

- (b) We have carried out a numerical analysis of the influence of the triangle-loop diagram by comparing the size of the diagrams in Fig. 10.

Our findings are: the amplitude of diagram (b) in Fig. 10 is suppressed by two orders of magnitude with respect to the amplitude of diagram (a) in Fig. 10 (we have here not included the additional suppression due to the gluon coupling constant). The influence of the third type of diagrams, also much smaller than diagram (a) in Fig. 10, is absorbed in the gluon vertex renormalization and therefore does not concern us. Adding extra gluon exchanges does not substantially change this picture. As a result we come to the conclusion that, in low orders of g_s , tree-diagrams are suppressed with respect to ladder-type diagrams.

We now consider photoproduction of the para state. The class of diagrams we have to compare are shown in Fig. 11. The importance of these diagrams is estimated by the following chain of arguments:

- (a) Both diagrams are cut along the dashed lines and the size of the remaining amplitudes on the left hand side will be estimated and compared.
- (b) We have mentioned earlier that the size of the triangle-loop diagram (Fig. 10b) has been estimated with respect to the single gluon exchange diagram (Fig. 10a); it is suppressed by two orders of magnitude in amplitude.

(c) The differential cross section resulting from the diagram in Fig. 10b is 4 orders of magnitude below single gluon exchange in Fig. 10a which means: $\left(\frac{d\sigma}{dt}\right)_{\text{triangle}} \approx 10^{-2} \text{ nb/GeV}^2$. The corresponding value for diagram Fig. 11a (left of dashed line) is determined using Fig. 3a: $\left(\frac{d\sigma}{dt}\right)_{\text{two-gluon}} \approx 1-10 \text{ nb/GeV}^2$. We thus conclude that the contribution of diagram (a) is substantially more important than diagram (b). (Fig. 11).

Our findings are: tree-diagrams contribute in η_c photoproduction in the same order of g_s as ladder-type diagrams. However their contribution is orders of magnitudes below the ladder diagrams considered above. Note that this result does not substantially change if α_s grows or the quark mass is changed.

VIII. CONCLUSION

In this paper we have presented an analysis of photoproduction of a heavy fermion pair assuming that it interacts via a long range gluon potential with the target nucleon. Within the framework of the Cheng-Wu picture a theory has been developed for para and ortho quark-pair production assuming that gluons are responsible for the interaction with the target. The characteristics of the resulting angular distributions have been determined; in particular the sizes and shapes of 3 and 3, 5, ... gluon exchanges for para production and 2 and 2, 4, ... gluon exchanges for ortho production was found. The angular distribution for η_c production is predicted to be flat and the cross section in the nanobarn range whereas it exponentially decreases in the case of ψ_c photoproduction. We also were able to show that diagrams with three or more gluons attached to each other (gluon-trees) may safely be neglected. The theory also has been applied to photoproduction of an unbound $\tau^+ \tau^-$ pair where multiphoton exchanges were found to enhance the cross sections by a factor 2-3.

Acknowledgments

I would like to thank Fred Gilman for his reading of the manuscript and clarifying discussions and Peter Lepage for his improvements of the text. Inspiring and clarifying conversations with Peter Lepage, Henry Tye, Hannu Miettinen, Peter Scharbach and Profs. C. Schmid and D. Horn are gratefully acknowledged. I am grateful to Prof. S. D. Drell for his warm hospitality and for the opportunity to work in the stimulating atmosphere of SLAC.

REFERENCES

1. H. Fritzsch, M. Gell-Mann and H. Leutwyler, Phys. Lett. 47B, 365 (1973). S. Weinberg, Rev. Mod. Phys. 46, 255 (1974). W. Marciano and H. Pagels, Rockefeller University preprint "Quantum Chromo Dynamics," No. COO-2232B-130. B. Humpert, "QCD—A Viable Theory of Strong Interactions?" (to appear).
2. F. E. Low, Phys. Rev. D 12, 163 (1975). S. Nussinov, Phys. Rev. Lett. 34, 1286 (1975); Phys. Rev. D 14, 246 (1976). T. Appelquist and H. D. Politzer, Phys. Rev. Lett. 34, 43 (1975).
3. S. J. Brodsky and J. F. Gunion, Phys. Rev. Lett. 37, 402 (1976).
4. S. J. Brodsky, R. Blankenbecler, and J. F. Gunion, Stanford Linear Accelerator Center preprint SLAC-PUB-1938.
5. J. Ellis, M. K. Gaillard, and G. Ross, Nucl. Phys. B111, 253 (1976).
6. S. D. Drell, Stanford Linear Accelerator Center preprint SLAC-PUB-1683 (1975). H. Joos, DESY preprint 76/36 (1976). S. Yankielowicz, Stanford Linear Accelerator Center preprint SLAC-PUB-1800 (1976).
7. M. K. Gaillard, B. W. Lee, and J. L. Rosner, Rev. Mod. Phys. 47, 277 (1975).
8. A. De Rujula, "Newly Discovered Resonances," Harvard University (1976).
9. See for example, G. S. Abrams in Proc. Int. Symposium on Lepton and Photon Interactions at High Energies, Stanford University, edited by W. T. Kirk (Stanford Linear Accelerator Center, Stanford University, Stanford, California, 1975), p. 25. R. Prepost, ibid., p. 241. For a review see: B. Humpert, "Dynamical Concepts on Scaling Violation and the New Resonances in e^+e^- Annihilation," Lecture Notes in Physics 45 (Springer Verlag, Heidelberg, 1976).

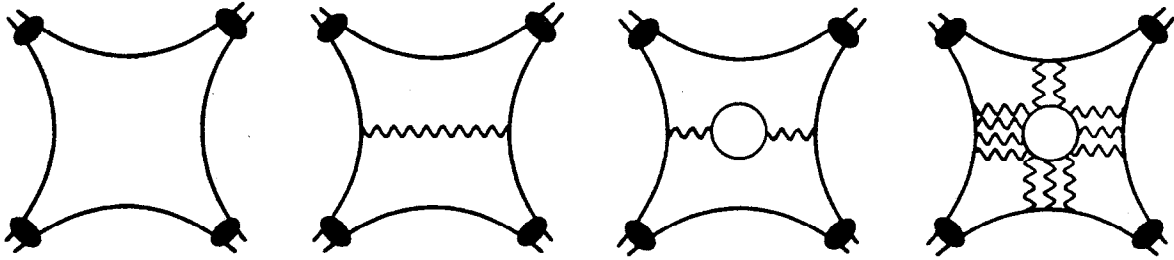
10. B. Humpert and A. C. D. Wright, Phys. Lett. 65B, 463 (1976); Phys. Rev. D 15, 2503 (1977); Stanford Linear Accelerator Center preprint SLAC-PUB-1831 (to be published in Ann. Phys.).
11. B. Humpert, Phys. Lett. 68B, 66 (1977).
12. H. Cheng and T. T. Wu, 1971 International Symposium on Electron and Photon Interactions at High Energies, Cornell University, Ithaca, New York (1971), p. 147 and Ref. 12.
13. R. Blankenbecler and R. L. Sugar, Phys. Rev. D 2, 3024 (1976); Phys. Rev. 183, 1387 (1969). S. J. Chang, "Diagrammatic Approach to Geometrical Models," preprint ILL-(Th-)76-13 (June 1976).
14. J. D. Bjorken, J. B. Kogut, and D. E. Soper, Phys. Rev. D 3, 1382 (1971); Phys. Rev. D 1, 2901 (1970). S. Brodsky, R. Roskies, and R. Suaya, Phys. Rev. D 8, 4576 (1973). J. Kogut and L. Susskind, Physics Reports 8C, 75 (1973).
15. I. J. Muzinich, E. A. Paschos, and D. P. Sidhu, BNL preprint (May 1976). A. Halprin and H. Primakoff, Phys. Rev. D 14, 1776 (1976). J. W. Moffat, Phys. Rev. Lett. 35, 1605 (1975).
16. H. D. Politzer, Harvard preprint HUTP-77/A029 and references therein.
17. H. D. Politzer, Physics Reports 14C, 130 (1974).
18. H. Cheng and T. T. Wu, Phys. Rev. 182, 1873 (1969); Phys. Rev. D 5, 3077 (1972); Phys. Rev. D 6, 2637 (1972).
19. S. D. Drell, D. J. Levy, and T. M. Yan, Phys. Rev. D 1, 1617 (1972).
20. L. I. Schiff, Quantum Mechanics (McGraw-Hill Book Co., New York, 1968).
21. H. Bethe and L. C. Maximon, Phys. Rev. 93, 768 (1954).
22. T. Faroszewicz and J. Wosiek, Munich preprint (unpublished).

23. W. Lee in Proc. Int. Symposium on Lepton and Photon Interactions at High Energies, Stanford University, edited by W. T. Kirk (Stanford Linear Accelerator Center, Stanford University, Stanford, California, 1975), p. 635.

FIGURE CAPTIONS

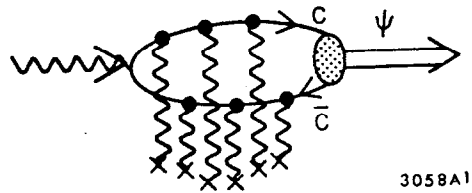
1. Quark interaction in gluon theories.
2. Three-step picture of $\psi(c\bar{c})$ photoproduction in the gluon potential of the nucleon.
3. (a) and (b) Photoproduction of ortho charmonium (ψ_c). The solid line represents 2, 4, 6, ... gluon exchange, the dashed line indicates the importance of 2-gluon exchange alone, whereas the dash-dotted line shows the cross section size of 4, 6, ... gluon exchange. The parameters are: $m_c = 1.5$ GeV and $\alpha_s = 0.5$ and $\alpha_s = 0.8$. (c) Photoproduction of an ortho $q\bar{q}$ state (ψ_q). The solid line, dashed line and dash-dotted line represent 2, 4, 6, ... gluon exchange. The parameters are: $m_q = 0.3$ GeV and $\alpha_s = 0.5$.
4. (a) and (b) Photoproduction of para charmonium (η_c). The solid line represents 3, 5, 7, ... gluon exchange, the dashed line indicates single gluon exchange (which is forbidden by color conservation!) and the dotted line indicates the size of the 3-gluon exchange near the forward direction. The parameters are: $m_c = 1.5$ GeV, $\alpha_s = 0.5$ and $\alpha_s = 0.8$. (c) Photoproduction of a para $q\bar{q}$ state (η_q). The solid line, dashed line and dotted line represent 3, 5, 7, ... gluon exchange, single-gluon exchange and 3-gluon exchange. The parameters are: $m_q = 0.3$ GeV and $\alpha_s = 0.5$.
5. (a) and (b) Photoproduction of a $\tau^+ \tau^-$ pair in an ortho (Fig. 5a) and para (Fig. 5b) state. The solid line represents 2, 4, 6, ... (1, 3, 5, ... , respectively) photon exchange whereas the dashed line indicates the size of 2 (1, respectively) photon exchange along. The nucleus charge is chosen to be $Z = 82$ and $m_\tau = 1.8$ GeV.
6. Gluon tree-diagrams which have been ignored in the model.
7. Cutting and opening of the fermion loop.

8. Ladder-type diagrams of order g_s^4 considered by the model.
9. Gluon tree-diagrams of order g_s^6 (a) and order g_s^8 (b).
10. Estimate of size of single gluon exchange diagram (a) versus the size of simplest gluon tree-diagram (b, c).
11. Estimate of size of ladder-type diagrams (a) versus size of tree-like gluon exchange diagrams (b, c).



3020A18

Fig. 1



3058A1

Fig. 2

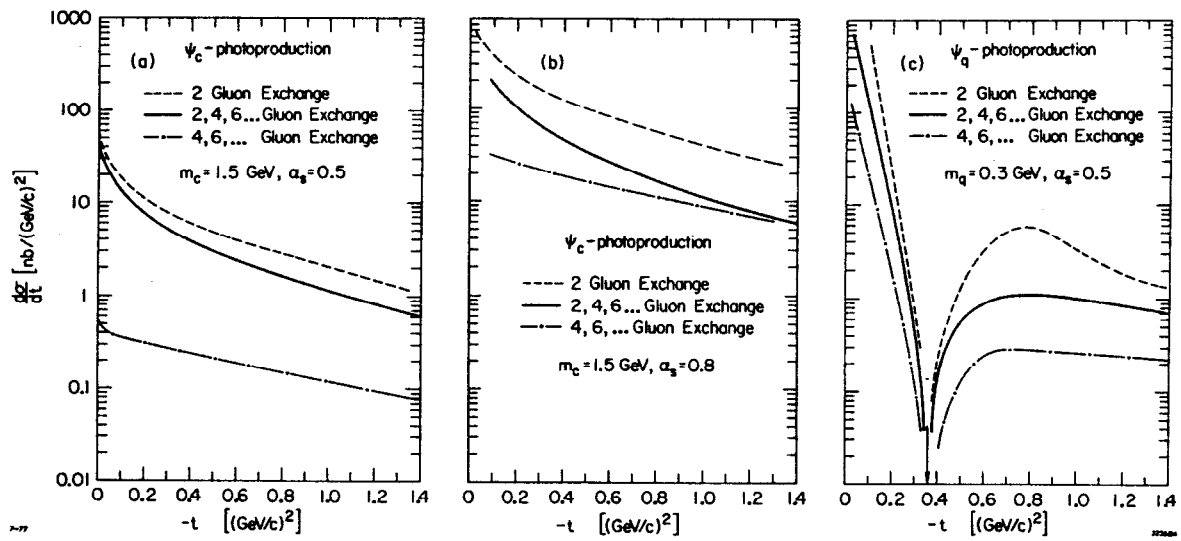


Fig. 3

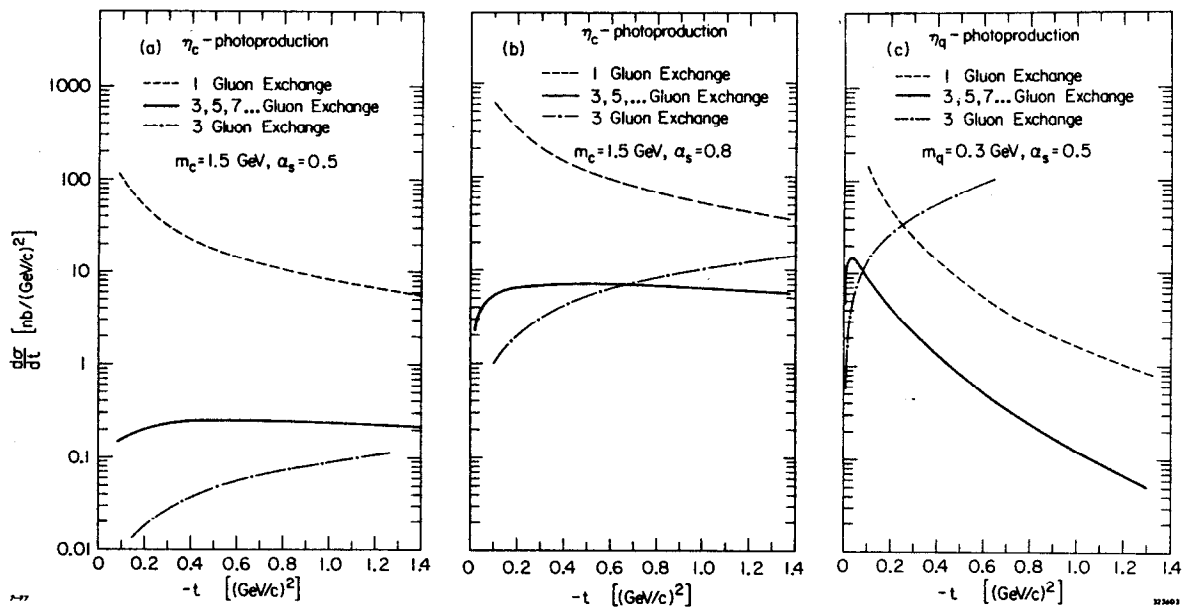


Fig. 4

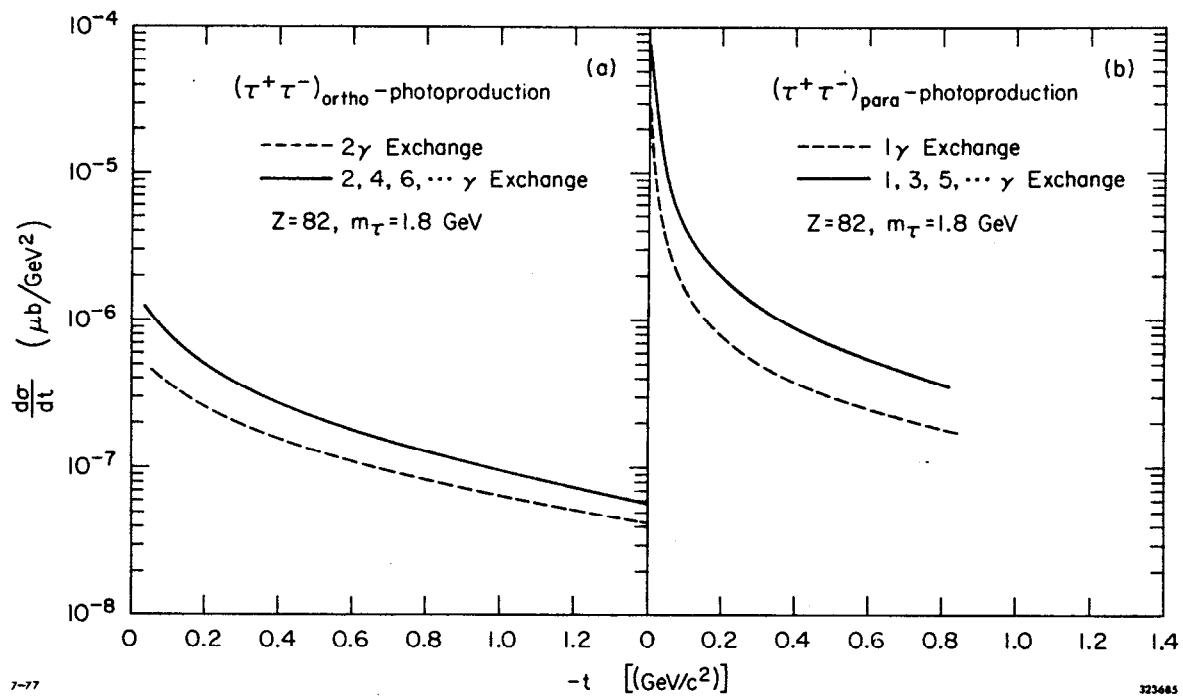
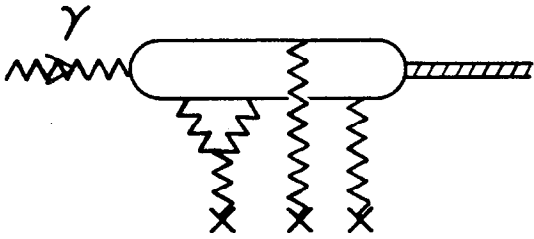
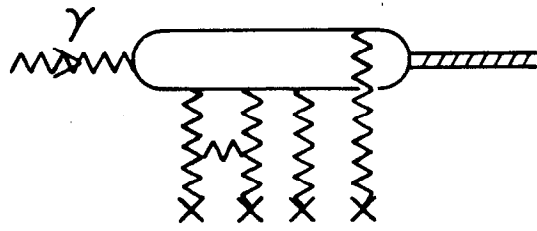


Fig. 5



(a)



(b)

7-77

3236A6

Fig. 6

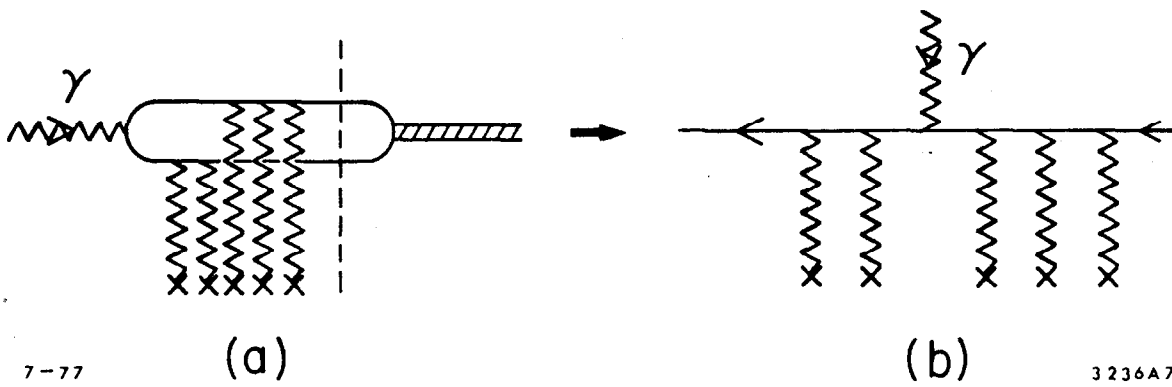


Fig. 7

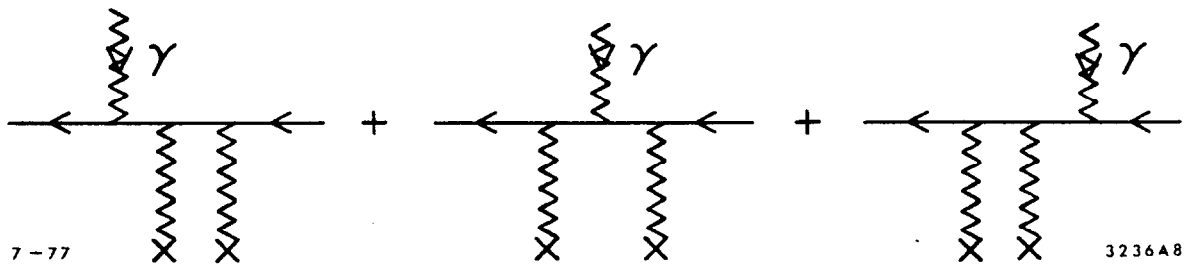
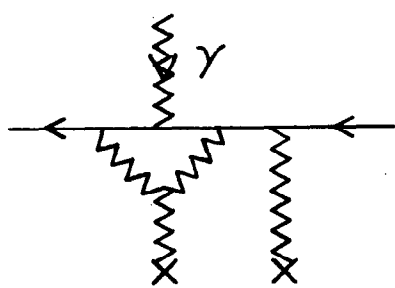
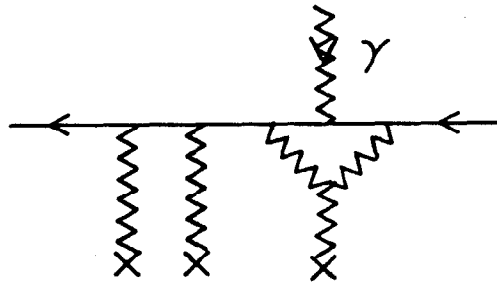


Fig. 8



7-77

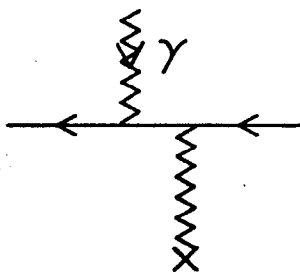
(a)



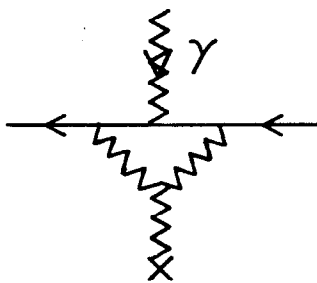
(b)

3236A9

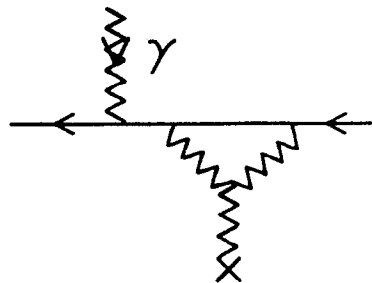
Fig. 9



7-77 (a)



(b)



(c)

3236A10

Fig. 10

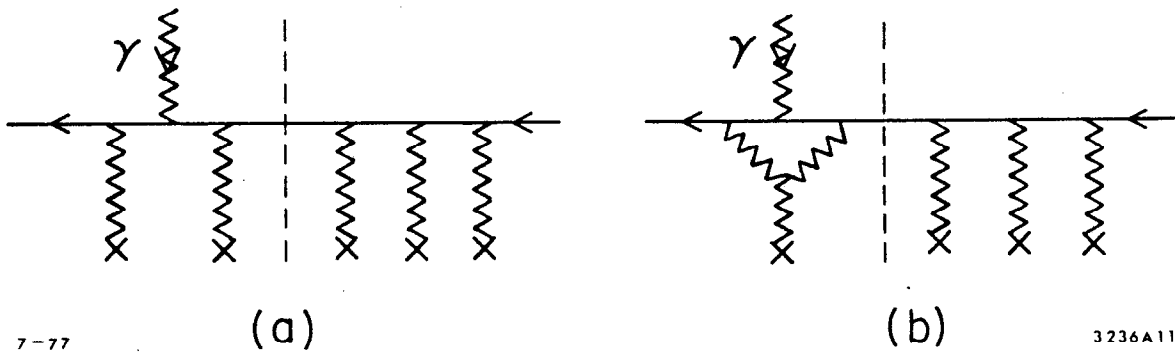


Fig. 11